EPJ Web of Conferences **123**, 02005 (2016) DOI: 10.1051/epjconf/201612302005
Heavy Ion Accelerator Symposium 2015

Conversion electrons from high-statistics β-decay measurements with the 8π spectrometer at TRIUMF-ISAC

P. E. Garrett[1,a], B. Jigmeddorj[1], A. J. Radich[1], C. Andreoiu[2], G. C. Ball[3], J. C. Bangay[1], L. Bianco[1,b], V. Bildstein[1], S. Chagnon-Lessard[1,c], D. S. Cross[2], G. A. Demand[1], A. Diaz Varela[1], R. Dunlop[1], P. Finlay[1,d], A. B. Garnsworthy[3], K. L. Green[1], G. Hackman[3], B. Hadinia[1], K. G. Leach[1,e], J. Michetti-Wilson[1], J. N. Orce[3,4], M. M. Rajabali[3,f], E. T. Rand[1], K. Starosta[2], C. Sumithrarachchi[1,g], C. E. Svensson[1], S. Triambak[3,4,5], Z. M. Wang[2,3], S. J. Williams[3,h], J. L. Wood[6], J. Wong[1], S. W. Yates[7], and E. F. Zganjar[8]

[1] *Department of Physics, University of Guelph, Guelph, ON N1G2W1 Canada*
[2] *Department of Chemistry, Simon Fraser University, Burnaby, BC V5A1S6 Canada*
[3] *TRIUMF, 4004 Wesbrook Mall, Vancouver, BC V6T2A3 Canada*
[4] *Department of Physics, University of the Western Cape, P/B X17, Bellville, ZA-7535 South Africa*
[5] *iThemba LABS, P.O. Box 722, Somerset West 7129, South Africa*
[6] *School of Physics, Georgia Institute of Technology, Atlanta, Georgia 30332, USA*
[7] *Departments of Chemistry and Physics & Astronomy, University of Kentucky, Lexington, Kentucky 40506, USA*
[8] *Department of Physics and Astronomy, Louisiana State University, Baton Rouge, Louisiana 70808, USA*

Abstract. The 8π spectrometer, located at TRIUMF-ISAC, was the world's most powerful spectrometer dedicated to β-decay studies until its decommissioning in early 2014 for replacement with the GRIFFIN array. An integral part of the 8π spectrometer was the Pentagonal Array for Conversion Electron Spectroscopy (PACES) consisting of 5 Si(Li) detectors used for charged-particle detection. PACES enabled both $\gamma - e^-$ and $e^- - e^-$ coincidence measurements, which were crucial for increasing the sensitivity for discrete e^- lines in the presence of large backgrounds. Examples from a ^{124}Cs decay experiment, where the data were vital for the expansion of the ^{124}Cs^m decay scheme, are shown. With sufficient statistics, measurements of conversion coefficients can be used to extract the $E0$ components of $J^\pi \rightarrow J^\pi$ transitions for $J \neq 0$, which is demonstrated for data obtained in ^{110}In$\rightarrow^{110}$Cd decay. With knowledge of the shapes of the states involved, as obtained, for example, from the use of Kumar-Cline shape invariants, the mixing of the states can be extracted.

1 Introduction

Prior to its decommissioning, the 8π spectrometer, located at the TRIUMF-ISAC radioactive beam facility in Vancouver, Canada, was the world's most powerful HPGe array routinely used for β-decay studies. This status was achieved because the spectrometer and its auxiliary detector systems were dedicated to β-decay studies only, allowing it to be optimized for that singular purpose. The 20 Compton-suppressed HPGe γ-ray detectors were configured in a truncated icosahedral geometry and achieved $\approx$ 1% photopeak efficiency at the energies of the ^{60}Co γ rays. Surrounding the beam-implantation point onto a FeO or Al coated mylar tape of the Moving Tape Collector at the center of a vacuum chamber were up to 20 plastic scintillator detectors of the SCintillating Electron-Positron Tagging Array (SCEPTAR). A different configuration involved the removal of the upstream hemisphere of SCEPTAR and its replacement with the Pentagonal Array for Conversion Electron Spectroscopy (PACES). Finally, the downstream SCEPTAR hemisphere could be removed and replaced with a single fast-plastic scintillator. These detector systems were coupled to a high-throughput and high-precision data acquisition system capable of triggering in excess of 30 kHz that enabled the collection of high-statistics data sets in a reasonable amount of beam time, but also enabled the half life and branching ratio measurements to a level of precision of better than 0.1% required for studies of Fermi superallowed β^+ emitters. Additional details of the spectrometer can be found in Refs. [1–3].

[a] e-mail: pgarrett@physics.uoguelph.ca
[b] present address: DESY Photon Science, Notkestrasse 85 D-22607 Hamburg, Germany
[c] Present address: Department of Physics, University of Ottawa, 150 Louis-Pasteur, Ottawa, ON K1N 6N5, Canada
[d] Present address: Instituut voor Kern-en Stralingsfysica, K.U. Leuven, Celestijnenlaan 200D, B-3001 Leuven, Belgium
[e] Present address: Department of Physics, Colorado School of Mines, Golden, Colorado 80401, USA
[f] Present address: Department of Physics, Tennessee Technological University, Cookeville, Tennessee 38505, USA
[g] Present address: National Superconducting Cyclotron Laboratory, Michigan State University, 640 South Shaw Lane, East Lansing, Michigan 48824, USA
[h] Present address: Diamond Light Source Ltd., Diamond House, Harwell Science and Innovation Campus, Didcot, Oxfordshire OX11 0DE, United Kingdom

The 8π spectrometer was decommissioned in the early part of 2014 and replaced with the much more powerful GRIFFIN array [1, 4]. Consisting of 16 large-volume HPGe clover detectors, GRIFFIN utilizes all of the existing auxiliary detectors and in addition can be coupled with the DESCANT neutron detector array [5] for studies of β-delayed neutron emitters.

One of the main goals of the science program carried out with the 8π spectrometer was the investigation of collectivity in nuclei, especially those located on or near the valley of stability. For these studies, high sensitivity to weak, low-energy γ-ray branches from highly-excited states is necessary. Studies to date have included, for example, the decay of ^{110}In [6–9], ^{112}In/^{112}Ag [10, 11], and ^{122,124,126}Cs [12, 13] into ^{110}Cd, ^{112}Cd, and ^{122,124,126}Xe, respectively. The 8π spectrometer proved itself a valuable tool for these studies since, for the above species, the high intensity of the radioactive beams delivered by TRIUMF more than compensated for the low absolute efficiency (by modern standards) for γ-ray detection.

In addition to the detection and measurement of weak γ-ray decay branches, in many of the experiments the 8π spectrometer was augmented with PACES for the purpose of conversion-electron detection and to seek possible $E0$ branches. As is well known, the measurement of $E0$ strengths, in the form of $\rho^2(E0)$ values, provides crucial information concerning the mixing of states with different intrinsic shapes. Such measurements, however, prove to be especially challenging requiring the ability to extract $E0$ branches in the presence of large backgrounds from β particles and Compton scattering of γ rays. Further, high statistics for $J^\pi \rightarrow J^\pi$ transitions with $J^\pi \neq 0$ must be acquired since the $M1/E2$ contribution to the electron intensity must be subtracted.

2 E0 conversion electron studies

$E0$ transitions are sensitive to the changes in the nuclear charge-squared radii since the $E0$ operator is [14]

$$\hat{M}(E0) = \sum_i e_i r_i^2, \tag{1}$$

where the sum extends over the A bodies in the nucleus with their charges e_i and radial position r_i. The usual quantity quoted when referring to an $E0$ transition is the $\rho^2(E0)$ value, defined via [14]

$$\Gamma(E0) = \frac{1}{\tau(E0)} = \rho^2(E0) \sum_j \Omega_j(Z, \Delta E), \tag{2}$$

where $\Gamma(E0)$ is the partial width for the decay, $\tau(E0)$ the partial lifetime, and $\Omega(Z, E_e)$ the electronic factor that depends on the atomic number Z and the energy of the transition ΔE. The quantity $\rho(E0)$ is defined by, with $R = 1.2A^{1/3}$ fm,

$$\rho(E0) = \frac{1}{eR^2} \left\langle I_f \left| M(E0) \right| I_i \right\rangle, \tag{3}$$

and carries all of the nuclear structure information. A successful measurement of the $\rho^2(E0)$ value thus requires a measurement of the branching fraction of the total transition intensity that proceeds through the $E0$ decay, i.e.,

$$BR(E0) = \frac{I(E0)}{\sum_i I_i(\gamma) + I_i(e^-)}, \tag{4}$$

where the summation extends over all possible branches (neglecting very small possible contributions from two-photon decay, internal pair formation, etc.) and also a measurement of the level lifetime τ. The number of $\rho^2(E0)$ values known is still rather limited [14, 15].

The $\rho^2(E0)$ values can be expressed in terms of the collective variables from the Bohr model. The operator is [16]

$$\hat{M}(E0) = \frac{3Z}{4\pi} \left(\frac{4\pi}{5} + \beta^2 + \frac{5\sqrt{5}}{21\sqrt{\pi}} \beta^3 \cos\gamma \right), \tag{5}$$

so that in a two-level mixing solution with quadrupole deformation parameters (β_1, γ_1) and (β_2, γ_2) the $E0$ strength is given by [14, 16]

$$\rho^2(E0) = \left(\frac{3Z}{4\pi} \right)^2 a^2 \left(1 - a^2\right) \left[\left(\beta_1^2 - \beta_2^2\right) + \frac{5\sqrt{5}}{21\sqrt{\pi}} \left(\beta_1^3 \cos\gamma_1 - \beta_2^3 \cos\gamma_2 \right) \right]^2. \tag{6}$$

The first term, proportional to the differences in the squares of the quadrupole deformation parameters β, is the usual expression that one sees for the $\rho^2(E0)$ values. The second term shows the leading order term involving the shape parameter γ; since it enters as the cube of the deformation β, its contribution is usually small. What is clear from Eqn. 6 is if information on the shape parameters β are known, the mixing of states can be determined.

3 The PACES Apparatus

PACES, shown in the photograph in Fig. 1, is installed internally in the vacuum chamber that is surrounded by the HPGe detectors of the 8π spectrometer. The 5 Si(Li) detectors have a 5 mm thickness, with a surface area of ≈ 200 mm^2, and are located at a distance of 3 cm from the beam deposition position. The Si(Li) detectors are in thermal contact with an Al plate that is cooled by an annular Cu cold finger of 0.75 m length. The annular cold finger is placed inside the beam line, with the annular opening allowing the beam to pass through. The Si(Li) detectors have a typical resolution of 2.5 keV at 1 MeV. The available active area of PACES covers $\approx 7\%$ of 4π solid angle, making it an efficient device for coincidence studies. Further details can be found in Refs. [1, 8].

4 Conversion electron spectroscopy with PACES

Inclusion of conversion-electron data may reveal not only $E0$ transitions, indicative of shape coexistence effects, but also provides multipolarity information. In studies of nuclei with a large number of levels at low-excitation energy,

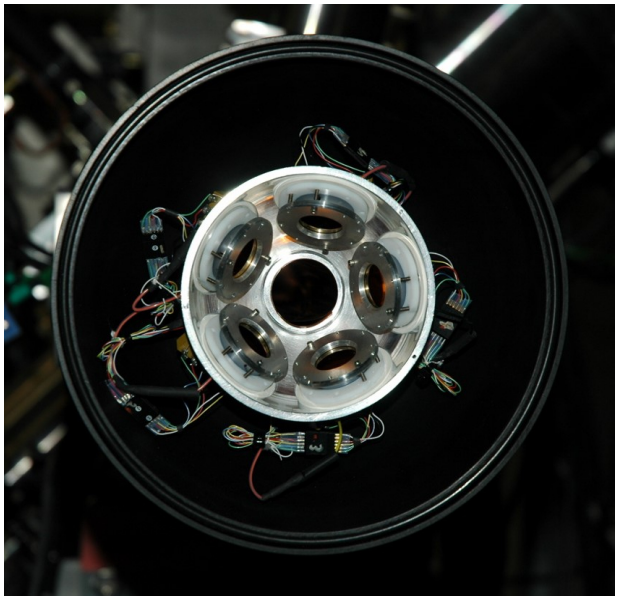

Figure 1. Photograph showing the detail of the PACES array of Si(Li) detectors located on the upstream side of the vacuum chamber of the 8π spectrometer. Details of the positioning are listed in Ref. [8].

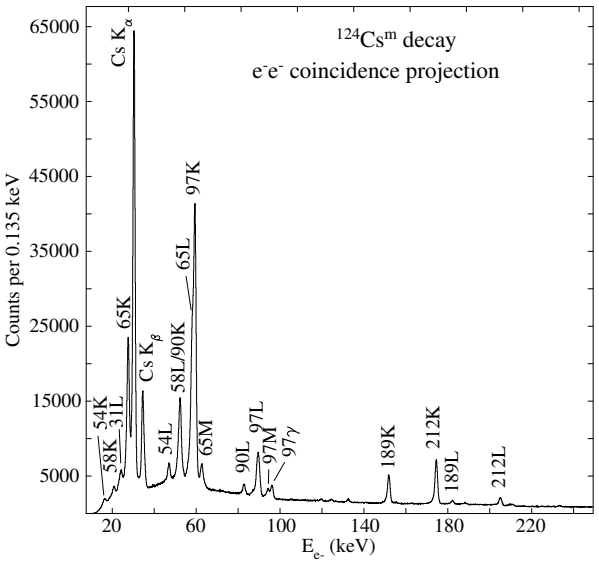

Figure 3. Projection of the $e^- - e^-$ coincidence matrix obtained during a measurement of the decay of ^{124}Cs^{m}.

as is often encountered in odd-odd nuclei or in the actinide region, the ability to detect low-energy conversion electrons and γ rays is vital in the construction of accurate decay schemes.

As mentioned above, a limitation on the measurement of $E0$ transitions, for $J \neq 0$ states, is that both the background level and the contribution of the $M1/E2$ electrons to the observed intensity of the transition must be subtracted. This requires much higher statistics than a measurement of the $0^+ \rightarrow 0^+$ transitions. Figure 2 displays a spectrum observed with the Si detectors of PACES in a recent measurement of the ^{124}Cs β^+/EC decay [13]. The sudden increases in the level of the background observed at 210 keV and 340 keV are Compton edges from intense 354-keV γ rays and the 511-keV annihilation radiation.

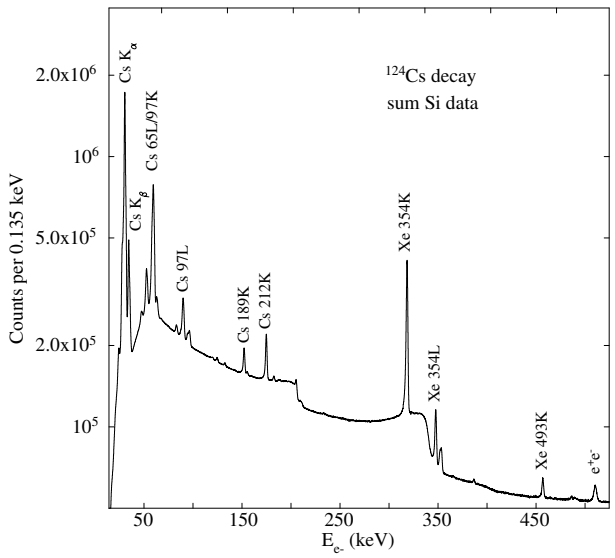

Figure 2. Example of a spectrum of conversion electrons obtained with the Si detectors of the 8π spectrometer in the β^+/EC decay of ^{124}Cs. The background is due to β^+-particle interactions in the detector, as well as Compton-scattering of γ rays. The main discrete lines observed are from Cs X-rays, transitions from the internal decay of the ^{124}Cs 7^+ isomeric state, and the most intense transitions in ^{124}Xe.

The fact that PACES consists of multiple, independent Si detectors enables $e^- - e^-$ coincidence spectroscopy. During a portion of a measurement to study the decay of ^{124}Cs, the observation of the decay of the $t_{1/2}$ = 6.3-s (7^+) ^{124}Cs isomeric state was enhanced relative to the $t_{1/2}$ = 30.8-s 1^+ ground state by employing a beam-on and tape movement cycling consisting of 1 s of beam implantation followed by 12 s of decay. This cycling minimized the build-up of the longer-lived ground state on the collection tape. Figure 3 shows the projection of the $e^- - e^-$ coincidence matrix collected during this portion of the experiment. Compared with data presented in Fig. 2, which was obtained using a beam/tape cycling appropriate for the long-lived ^{124}Cs ground state, the background in Fig. 3 is much lower due to the lower relative intensities of the high-energy γ rays in ^{124}Xe and the β^+ particles. Figure 4 displays $e^- - e^-$ coincidence spectra from gates with the 65-keV M conversion electrons (top panel) and 97-keV L electrons (bottom panel) from the ^{124}Cs isomer decay. Of particular note is the presence in the bottom panel of the 25-keV peak from the 31-keV L conversion electron, clearly resolved from the Cs K_α X-ray; the 31-keV transition was previously unobserved. Using data such as this, the decay scheme of the ^{124}Cs isomer was significantly modified and is shown in Fig. 5.

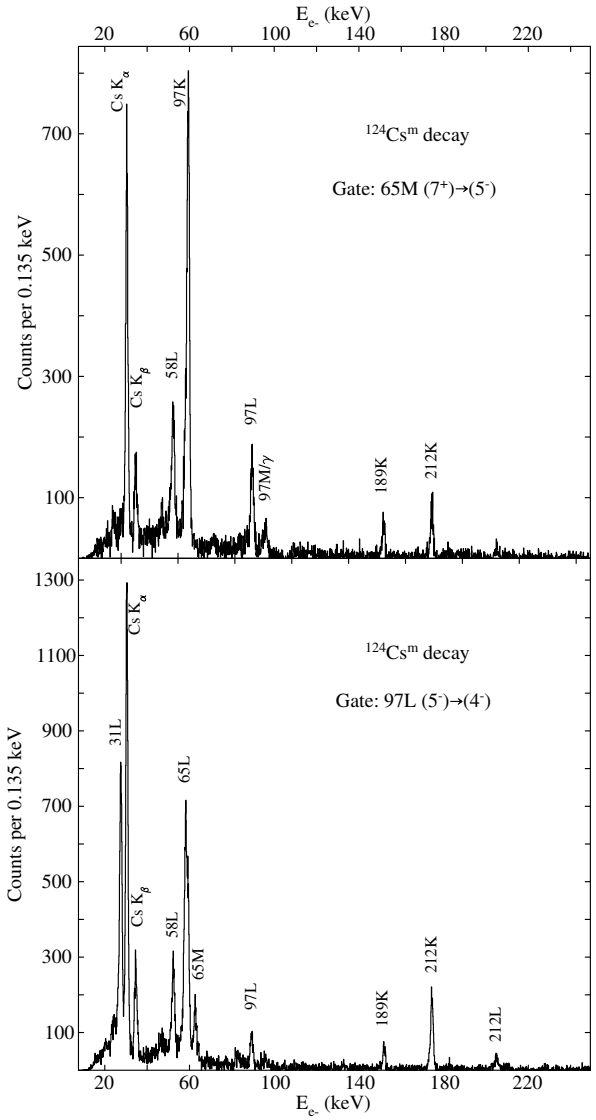

Figure 4. Examples of $e^- - e^-$ coincidence spectra from the decay of ^{124}Cs^m. The top panel displays the coincidence spectrum with a gate taken on the 65-keV M conversion electron peak, whereas the bottom panel displays the coincidence spectrum with the 97-keV L conversion electron peak. The 97-keV L gate includes a small contribution from the 90-keV γ-ray photopeak.

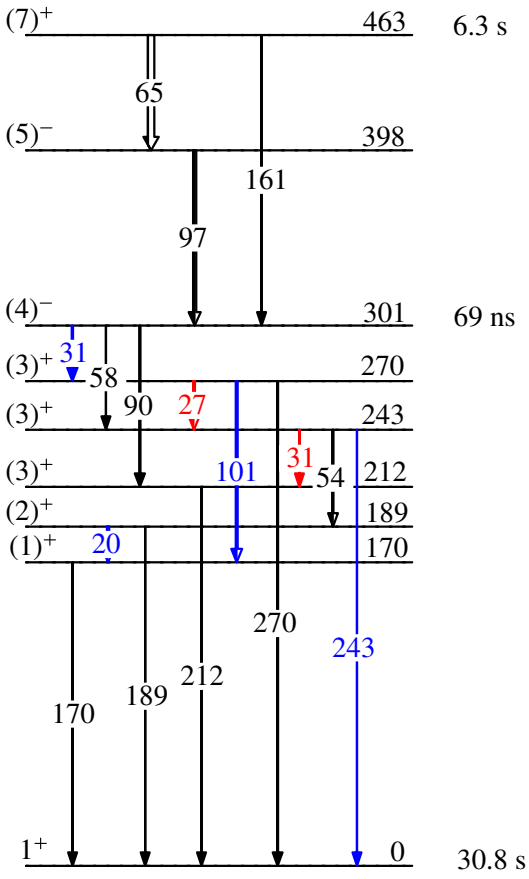

Figure 5. Level scheme deduced for the isomeric decay of ^{124}Cs^m. Levels are labelled with their energies in keV, and their J^π values. The transitions are labelled with their energies in keV. Arrows in blue are previously unobserved transitions in the decay of the isomer, with those in red new transitions.

5 E0 transitions in ^{110}Cd

A high-statistics data set for the decay of ^{110}In→^{110}Cd was collected with the dual goals of measuring weak, low-energy γ-ray decay branches from highly-excited states, and observing additional $E0$ branches. The high-intensity ion beam of 1.2×10^7 ions/s of ^{110}In in the 7^+ ground state with a 4.9-hr half life, and 1.7×10^6 ions/s of ^{110}In in the 2^+ isomeric state with a 69-min half life was delivered to the center of the 8π spectrometer.

The internal conversion coefficients were extracted from the $\gamma - e^-$ and $\gamma - \gamma$ coincidence data. The γ-ray coincidence gates were taken from above or below the decay of interest. When gating from below, the number of $\gamma - e^-$ coincident counts measured can be expressed as

$$N_{\gamma e^-} = KI^f_{e^-}\epsilon^f_{e^-}BR^d_\gamma\epsilon^d_\gamma\epsilon_c\eta(\theta_{\gamma e^-}), \quad (7)$$

where K is an overall normalization factor, I_{e^-} is the conversion electron intensity (f is the feeding and d the draining transition), ϵ_{e^-} is the detector efficiency for the conversion electron, ϵ_γ is the detector efficiency for the γ ray, BR_γ is the γ-ray branching ratio, ϵ_c is the coincidence efficiency and $\eta(\theta_{\gamma e^-})$ is an angular correlation factor. The number of $\gamma-\gamma$ coincident counts can be similarly written as

$$N_{\gamma\gamma} = KI^f_\gamma\epsilon^f_\gamma BR^d_\gamma\epsilon^d_\gamma\epsilon_c\eta(\theta_{\gamma\gamma}), \quad (8)$$

where I_γ is the γ-ray intensity. Rearranging for the intensity of γ rays and the intensity of conversion electrons from Eqns. 7 and 8, the internal conversion coefficient, in accordance with its definition, can be written as

$$\alpha = \frac{I^f_{e^-}}{I^f_\gamma} = \frac{N_{\gamma e^-}}{N_{\gamma\gamma}}\frac{\epsilon^f_\gamma}{\epsilon^f_{e^-}}. \quad (9)$$

An internal efficiency calibration was adopted (see Fig. 4 in Ref. [9]), using the conversion coefficients for well-

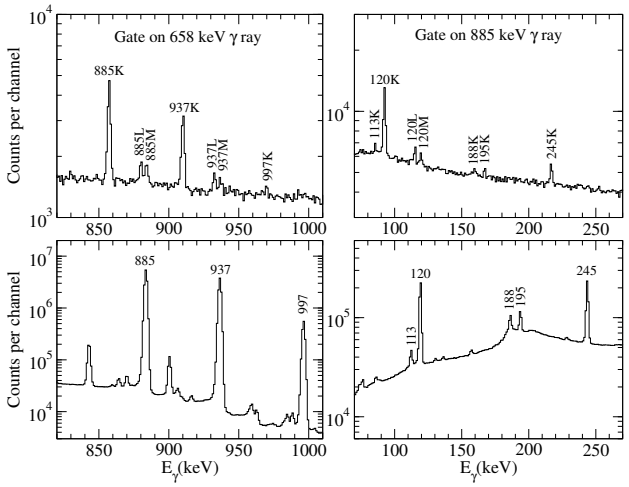

Figure 6. Portions of the conversion electron spectra in coincidence with the 658-keV $2_1^+ \rightarrow 0_{gs}^+$ (left) and 885-keV $4_1^+ \rightarrow 2_1^+$ (right) γ rays (top), and corresponding portions of the γ-ray coincidence spectra (bottom).

known $E2$ and $E1$ transitions or those determined in the present work to be essentially pure $M1$ or $E2$ transitions.

Shown in the top panel of Fig. 6 are examples of partial e^- spectra obtained by placing coincidence gates on the 658- (left) and 885-keV (right) γ rays. The bottom panel displays the corresponding γ-ray coincidence spectra with the same γ-ray coincidence gates applied. Fitting of the corresponding electron and γ-ray peaks provides the number of coincidence counts used in Eqn. 9.

Figure 7 shows portions of the e^- spectra with coincidence gates taken on the 245- and 626-keV γ rays. These particular spectra display the K-conversion electron lines from the 708-keV $4_3^+ \rightarrow 4_1^+$ transition and the 397-keV $6_2^+ \rightarrow 6_1^+$ transition that connect the deformed intruder band, based on $\pi(2p-4h)$ configuration, to the less deformed "normal" states. The extracted $\rho^2(E0)$ values for the $E0$ transitions, which includes the new value for the 708-keV $4_3^+ \rightarrow 4_1^+$ transition of $\rho^2(E0) = 106^{+98}_{-91} \times 10^{-3}$, are shown in Fig. 8.

6 Implications of ρ^2(E0) values

As shown in Eqn. 6, the determination of experimental $\rho^2(E0)$ values enables the admixtures between states to be determined provided that the underlying intrinsic shapes are known. In many cases this is not possible since the shapes have typically not been determined for excited states. However, when Coulomb excitation has been performed with sufficient sensitivity and statistics such that the Kumar-Cline [17, 18] shape invariants can be constructed, the shapes of the states can be extracted in a model-independent way. Such a case is ^{114}Cd [19].

The Coulomb excitation experiment performed by Fahlander *et al.* [19] provided a sufficient number of matrix elements that enables the shape invariant Q^2 to be de-

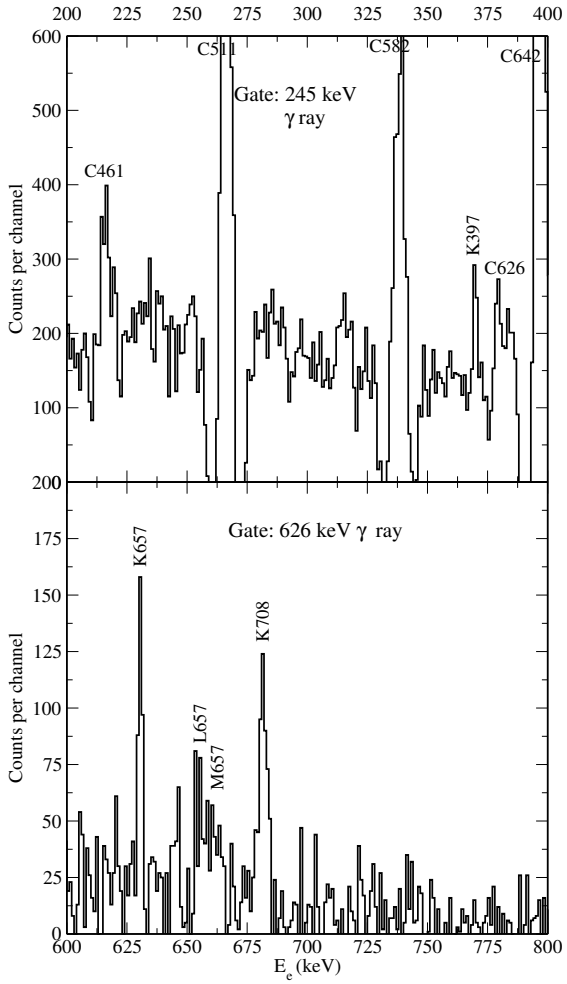

Figure 7. Portions of the spectra of the conversion electrons in coincidence with the 245- (top) and 626-keV (bottom) γ rays. The coincidence with the 245-keV γ ray shows the 397-keV K-conversion electron peak, which is weak, and some much stronger peaks that result from Compton scattering of the 511-keV annihilation radiation and the 582- and 642-keV γ rays. The coincidence spectrum with the 626-keV γ ray shows the 708-keV K-conversion electron peak.

termined from

$$\frac{1}{\sqrt{5}}Q^2 = \frac{(-1)^{2I_i}}{\sqrt{2I_i+1}} \sum_j \langle I_i||\mathcal{M}(E2)||I_j\rangle \times \langle I_j||\mathcal{M}(E2)||I_i\rangle \begin{Bmatrix} 2 & 2 & 0 \\ I_i & I_i & I_j \end{Bmatrix}, \quad (10)$$

where $\mathcal{M}(E2)$ is the transition matrix element and $\{\}$ is a $6j$ symbol. While the sum extends over the complete set of states I_j, it generally is determined by a few key matrix elements. The Q^2 invariant extracted from the experimental data, $\langle Q^2\rangle$, can be related to the β shape parameter

$$\langle Q^2\rangle = q_0^2\langle\beta^2\rangle, \quad (11)$$

with $q_0 = \frac{3}{4\pi}ZR_0^2$ with $R_0 = 1.2A^{\frac{1}{3}}$ fm. Focusing on the ground state and the 0^+ intruder band head, $\langle Q^2\rangle$ parameters extracted [19] from the data are 0.53(1) and 1.1(1)

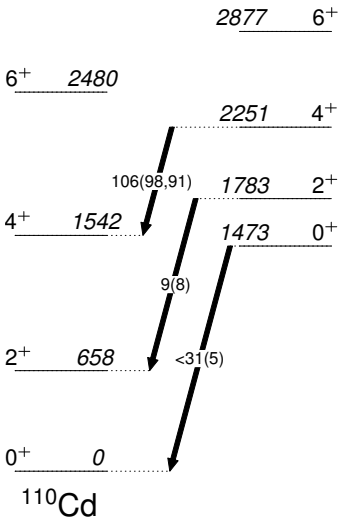

Figure 8. Partial level scheme for ^{110}Cd showing the $\rho^2(E0)\cdot 10^3$ values for transitions from the deformed intruder band to the ground-state band. The upper limit for the $0^+ \rightarrow 0^+$ transition is due to a lower limit on the lifetime for the 1473-keV 0^+ level.

e^2b^2, respectively, leading to $\langle\beta\rangle$ values of 0.187(2) and 0.27(1). In ^{114}Cd, $\rho^2(E0; 0_2^+ \rightarrow 0_1^+) = (19 \pm 2) \times 10^{-3}$, and with the above values of β, Eqn.6 leads to an admixture of $a^2 = 0.08$ of the intruder 0^+ wave function in the ground state.

7 Conclusions

Conversion electron spectroscopy is a powerful tool for the elucidation of level schemes, especially those involving highly-converted, low-energy transitions that are not always observed with γ-ray detectors. Furthermore, they provide a way to measure the $E0$ components of $J^\pi \rightarrow J^\pi$ transitions. The PACES array, employed at TRIUMF-ISAC with the 8π and GRIFFIN spectrometers, has provided such data. Examples of electron data from the decay of ^{124}Cs^m have been given that led to a modification of the decay scheme of this isomer. Data from the decay of ^{110}In were used to extract new $E0$ values, and a new $\rho^2(E0)$ value was determined for the decay of the 4^+ deformed intruder band to the 4^+ member of the ground-state band. Combining data from a previous Coulomb excitation study of ^{114}Cd with the available $\rho^2(E0)$ values permitted the admixture of the intruder 0^+ state in the ground state to be determined.

Acknowledgements

This work was supported in part by the Natural Sciences and Engineering Research Council (Canada) and the U.S. National Science Foundation under Grant No. PHY-1305801. TRIUMF receives federal funding via a contribution agreement through the National Research Council of Canada.

References

[1] P. E. Garrett *et al.*, J. Phys. Conf. Ser. **639** 012006 (2015).
[2] P. E. Garrett *et al.*, Nucl. Instrum. Meth. B **261** 1084 (2007).
[3] A. B. Garnsworthy and P. E. Garrett, Hyper. Int. **225** 121 (2014).
[4] C. E. Svensson and A. B. Garnsworthy, Hyper. Int. **225** 127 (2014).
[5] P. E. Garrett, Hyper. Int. **225** 137 (2014).
[6] P. E. Garrett *et al.*, Phys. Rev. C **86** 044304 (2012).
[7] A. Diaz Varela, P. E. Garrett, G. C. Ball *et al.*, E. Phys. J. Conf. **66** 02029 (2014).
[8] B. Jigmeddorj, P. E. Garrett, A. Diaz Varela *et al.*, JPS Conf. Proc. **6** 030014 (2015).
[9] B. Jigmeddorj, P. E. Garrett, A. Diaz Varela *et al.*, Eur. Phys. J. **A52**, 36 (2016).
[10] K. L. Green, P. E. Garrett, R. A. E. Austin *et al.*, Phys. Rev. C **80** 032502 (2009).
[11] P. E. Garrett, K. L. Green, R. A. E. Austin *et al.*, Acta Phys. Pol. **B42** 799 (2011).
[12] B. Jigmeddorj, P. E. Garrett, C. Andreoiu *et al.*, E. Phys. J. Conf. **107** 03014 (2016).
[13] A. J. Radich *et al.* Phys. Rev. C **91** 044320 (2015).
[14] J. L. Wood, E. F. Zganjar, C. De Coster, and K. Heyde, Nucl. Phys. **A651** 323 (1999).
[15] T. Kibédi, and R. H. Spear, Atom. Data Nucl. Data Tables **89** 77 (2005).
[16] J. P. Davidson, Rev. Mod. Phys. **37**, 105 (1965).
[17] K. Kumar, Phys. Rev. Lett. **28**, 249 (1972).
[18] D. Cline, Ann. Rev. Nucl. Part. Sci. **36**, 683 (1986).
[19] C. Fahlander, A. Bäcklin, L. Hasselgren*et al.*, Nucl. Phys. **A485** 318 (1988).